UDK 546.62:621.791.1
Original scientific article/Izvirni znanstveni članek

ISSN 1580-2949
Mater. Tehnol.

ENHANCED MECHANICAL PERFORMANCE AND REFINED INTERMETALLIC LAYER IN UNDERWATER FRICTION-STIR-WELDED AA5083–Cu DISSIMILAR JOINTS

IZBOLJŠANJE MEHANSKE ZMOGLJIVOSTI ZVARNIH SPOJEV ZA PODVODNE APLIKACIJE TER IZBOLJŠANJE LASTNOSTI INTERMETALNE PLASTI ZVAROV NA OSNOVI Al ZLITINE AA5083 IN Cu

P. R. Kannan[1*], N. Premkumar[2], M. Arul[3], S. Dinesh[4]

[1]Department of Mechanical Engineering, Mahendra Institute of Technology, Namakkal, Tamil Nadu, India 637503
[2]Department of Mechanical Engineering, SRM Institute of Science and Technology, Kattankulathur, Chennai, Tamil Nadu, India 603203
[3]Department of Mechanical Engineering, ARM College of Engineering and Technology, Chennai, Tamil Nadu, India 603209
[4]Department of Mechanical Engineering, Dhanalakshmi College of Engineering, Chennai, Tamil Nadu, India 601301

Prejem rokopisa – received: 2025-08-13; sprejem za objavo – accepted for publication: 2025-12-17

doi:10.17222/mit.2025.1550

This research investigates the underwater friction stir welding (UWFSW) of dissimilar AA5083 aluminum and pure-copper plates, aiming to enhance the mechanical performance through precise control of the process parameters and the suppression of excessive intermetallic compound (IMC) formation. The UWFSW was performed using a CNC vertical milling machine under full immersion to regulate the heat input and improve the joint's integrity. The optimized parameters yielded a maximum tensile strength of 7.5 MPa, impact strength of 7.5 J, and peak microhardness of 111 VH, outperforming conventional dry FSW joints. Optical microscopy and SEM analyses revealed a defect-free joint with a fine equiaxed grain structure in the stir zone, minimal deformation in the parent zones, and a uniform IMC layer of 2–5-μm thickness along the Al–Cu interface. The underwater cooling effect restricted grain coarsening and prevented void formation, resulting in enhanced metallurgical bonding. The study confirms that UWFSW offers a superior route to producing high-strength, corrosion-resistant Al–Cu dissimilar joints, making it highly suitable for marine, cryogenic, and high-performance electrical applications.

Keywords: underwater friction stir welding, AA5083 aluminum, pure copper, dissimilar joints, intermetallic compounds, mechanical properties, microstructural refinement, SEM analysis

V članku avtorji opisujejo raziskavo podvodnega trenjskega vrtilno-mešalnega varjenja (UWFSW; angl.: underwater friction stir welding) dveh težko oz. medseboj načeloma nezdružljivih kovin; i.e.: plošče iz Al zlitine tipa AA5083 in plošče iz tehniško čistega bakra (Cu). Namen raziskave je bil izboljšati mehanske lastnosti te vrste zvara s pomočjo natančne kontrole procesnih parametrov varjenja in zmanjšati pretiran nastanek neželjene intermetalne spojine (IMC; angl.: intermetallic compound). Za UWFSW postopek so uporabili vertikalno računalniško vodeni (CNC, angl.: Computer Numerical Control) rezkalni stroj s popolnim vodnim hlajenjem za kontrolo vnosa toplote in izboljšano integriteteto zvarnega spoja. Optimizirani parametri izbranega postopka varjenja so dali maksimalne vrednosti za natezno trdnost 7,5 MPa, udarno žilavost 7,5 J in maksimalno vrednost mikrotrdote 111 VH, kar močno presega vrednosti za zvarne spoje izdelane s konvencionalnim suhim trenjsko vrtilno-mešalnim varjenjem. Pregled pod svetlobnim in vrstičnim elektronskim mikroskopom je pokazal da so izdelani zvarni spoji brez napak z drobno enako-osno zrnato kristalno zgradbo v coni mešanja kovin, minimalno deformacijo v conah osnovnih kovin in homogeno IMC plastjo debeline med 2 μm in 5 μm vzdolž meje med Al zlitino in Cu. Učinek podvodnega hlajenja je omejil pretirano rast kristalnih zrn in nastanek praznin, kar je izboljšalo metalurško vez med izbranima nezdružljivima kovinama. Avtorji so s to raziskavo dokazali, da ponuja UWFSW postopek vrhunske možnosti za izdelavo zvarnih spojev iz načeloma nezdružljivih kovin, kot sta izbrana Al zlitina in Cu, ki imajo visoko trdnost in dobro korozijsko odpornost. Te vrste spojev pa so zelo primerne za pomorske, kriogene in visokozmogljive električne aplikacije.

Ključne besede: varjenje pod vodo, trenjsko vrtilno-mešalno varjenje, Al zlitina tipa AA5083, tehniško čist kovinski baker, zvarni spoji iz med seboj nezdružljivih kovin, mehanske lastnosti, izboljšanje mikrostrukture zvara, SEM analize

1 INTRODUCTION

The joining of dissimilar materials, particularly aluminum alloys and copper, has gained increasing industrial relevance due to the combined advantages of lightweight structures and superior electrical and thermal conductivity. AA5083 aluminum, a non-heat-treatable, corrosion-resistant alloy, and pure copper are widely employed in marine, cryogenic, and electrical systems where weight reduction, strength, and conductivity are critical. However, the conventional fusion welding of Al–Cu combinations often results in excessive heat input, the formation of brittle intermetallic compounds (IMCs), porosity, and distortion, leading to degraded mechanical properties.[1,2] Friction stir welding (FSW), as a solid-state process, offers a viable alternative by minimizing melting-related defects, but welding dissimilar Al–Cu joints remains challenging due to uneven thermal

*Corresponding author's e-mail:
drprkannan@gmail.com (P. R. Kannan)

conductivity, large differences in melting points, and uncontrolled IMC growth.[3,4]

Underwater friction stir welding (UWFSW) introduces a submerged environment that significantly enhances heat dissipation, suppresses excessive IMC formation, and reduces residual stresses.[5,6] Recent studies have demonstrated that underwater cooling produces narrower heat-affected zones, finer grains, and higher joint strength than conventional FSW.[7,8] However, most current UWFSW studies on Al–Cu joints either examine parameters in isolation, neglecting multi-response optimization, or lack statistically validated process design, resulting in limited repeatability and suboptimal mechanical performance. This represents a critical research gap where integrated mechanical, metallurgical, and statistical evaluations are needed to fully exploit the benefits of UWFSW for dissimilar welding.[9,10] Despite UWFSW's potential, reported AA5083–Cu welds frequently exhibit tensile strengths (60–120 MPa) far below the base material capabilities, primarily due to excessive or uneven IMC growth, insufficient thermal control, and non-optimized process parameters.[11,12] There is a need for a systematic optimization framework that enhances joint strength, ductility, and interfacial integrity while minimizing defects.

This work aims to develop and validate an optimized UWFSW process for AA5083–Cu dissimilar joints using a statistically robust Taguchi–VIKOR multi-response approach. The study systematically evaluates the influence of rotational speed, traverse speed, and tool-tilt angle on the tensile strength, hardness, and impact toughness, with three replicates per condition. The optimized joints are further examined through ASTM-compliant mechanical testing and detailed microstructural characterization to establish a process–structure–property relationship that ensures high-performance, defect-free dissimilar welds for marine, cryogenic, and electrical applications[13].

2 MATERIALS AND MANUFACTURING METHODS

2.1 Materials

In this study dissimilar butt joints were fabricated using AA5083-H116 aluminum alloy and commercially pure copper (Cu-ETP grade) plates, both with dimensions of (100 × 50 × 6) mm. AA5083 was selected due to its high strength-to-weight ratio, exceptional corrosion resistance in marine environments, and non-heat-treatable nature, which allows for microstructural refinement without the risk of over-aging during solid-state welding. Copper was chosen for its superior thermal and electrical conductivity, making the Al–Cu combination highly relevant for applications in marine heat exchangers, cryogenic systems, and electrical busbars. Both materials were procured from Go Green Pvt. Ltd., Chennai, Tamil Nadu, India, ensuring consistent chemical composition and mechanical properties in compliance with ASTM B209 (AA5083) and ASTM B152 (Cu) standards. A H13 tool-steel friction-stir-welding tool was used due to its

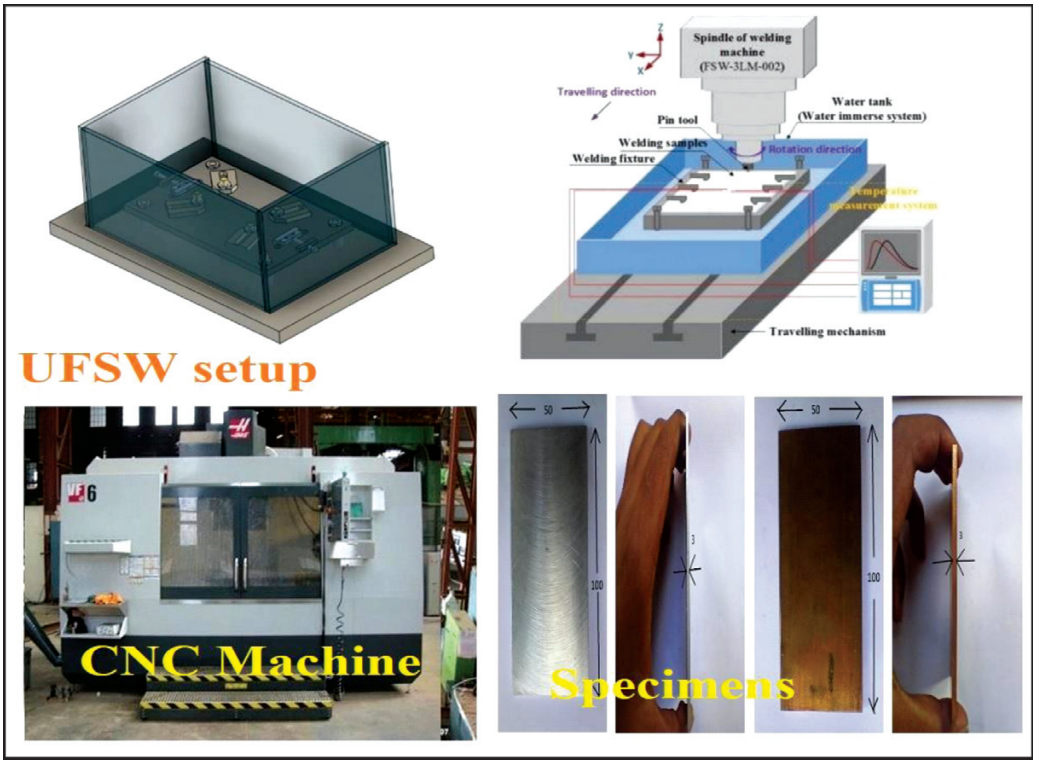

Figure 1: Specimen fabrication for underwater friction stir welding

high hot hardness, wear resistance, and thermal stability under the elevated temperatures and high-pressure conditions of UWFSW.[14,15] The tool consisted of a concave shoulder (18 mm diameter) and a threaded cylindrical pin (6 mm diameter, 5.7 mm length), designed to promote intense plastic flow and intermixing at the Al–Cu interface while minimizing defect formation. The selection of this material-tool configuration was based on its proven capability to withstand prolonged underwater operation without significant wear, as reported in recent UWFSW studies. The combination of AA5083 and Cu in an underwater environment is novel due to the complex thermal-mechanical interactions and the requirement to control IMC thickness within 1–3 μm for optimal joint performance—an objective rarely achieved in earlier dissimilar welding research.[16]

Figure 1 illustrates the complete specimen fabrication workflow for underwater friction stir welding (UWFSW) of AA5083–Cu joints. The top-left and top-right images show the design and schematic of the UWFSW setup, including the water-immersed fixture and CNC-controlled tool movement. The bottom-left image depicts the CNC vertical milling machine (HAAS VF-6) used to execute precise welding operations under submerged conditions. The bottom-right panel presents the prepared specimens, showing dimensions, surface finish, and joint interface, which are ready for mechanical testing. This integrated setup ensures controlled thermal input, precise alignment, and high repeatability, which are essential for producing reliable dissimilar welds in a submerged environment.

2.2 Manufacturing method

AA5083-H116 aluminum alloy and commercially pure copper (Cu-ETP) plates, each measuring (100 × 50 × 6) mm, were prepared for underwater friction stir welding (UWFSW). Before the welding, the faying surfaces were milled to ensure flatness within ±0.02 mm and degreased with acetone to remove contaminants that could inhibit metallurgical bonding. Edges were squared using a precision surface grinder to achieve full-contact butt alignment. The plates were then rigidly clamped on a stainless-steel backing plate to prevent distortion during welding. The welding trials were conducted on a model FSW-MAX-300 CNC-controlled friction stir welding machine (capacity: 30 kN downward force, 0–3000 min^{-1} spindle speed, 0–200 mm/min traverse speed) adapted for submerged operations within a temperature-controlled water tank. The tank maintained a water temperature of 25 ± 1 °C to ensure consistent cooling and suppression of excessive intermetallic compound (IMC) growth. The H13 tool steel welding tool featured a concave shoulder of 18 mm diameter and a threaded cylindrical pin of 6 mm diameter and 5.7 mm length, designed to promote effective material mixing at the Al–Cu interface. A Taguchi L9 orthogonal array was employed to systematically vary three process parameters: rotational speed (980, 1150, 1300) min^{-1}, traverse speed (20, 35, 40 mm/min), and tool tilt angle (0°, 1°, 3°). For each parameter combination, three replicate welds were produced to ensure statistical reliability. The tool plunge depth was set to 0.15 mm below the plate surface to ensure full penetration without shoulder-induced overheating. The welding process began with a dwell time of 3 s to establish plasticization, followed by steady-state welding under submerged conditions. The water medium acted as a heat sink, promoting finer grain structures and uniform IMC layers by limiting peak temperatures. After welding, specimens were removed, surface-oxidation deposits were cleaned mechanically, and samples were

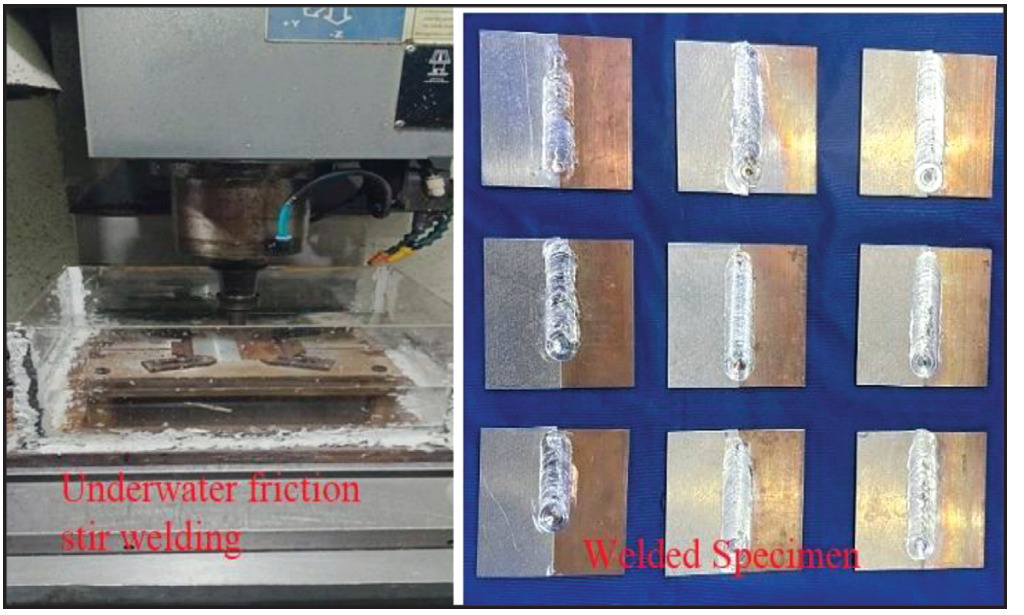

Figure 2: Underwater friction stir welding and welded specimens

Figure 3: Tensile test specimens before and after testing

coded (W1–W9) for subsequent mechanical and microstructural testing under ASTM standards.[17]

Figure 2 presents the underwater friction stir welding (UWFSW) process and the resulting welded AA5083–Cu dissimilar specimens. The left image captures the real-time welding operation conducted in a submerged environment using a CNC-controlled setup, effectively minimizing thermal gradients and oxidation. The right image showcases nine successfully fabricated welded specimens, each exhibiting uniform bead formation and consistent joint profiles, indicating effective material mixing and process stability. These results validate the capability of UWFSW to produce high-integrity, repeatable dissimilar joints under controlled thermal conditions.

3 EXPERIMENTAL TESTING

All the mechanical and microstructural evaluations were conducted in strict accordance with ASTM standards to ensure reliability, repeatability, and statistical robustness, addressing any concerns about test consistency. For each welding-parameter combination, three independent underwater friction stir welded (UWFSW) joints were produced, and two specimens were extracted from each weld where geometry permitted, providing a minimum of six replicates (n = 6) for each reported property. Sub-size flat tensile coupons (ASTM E8/E8M; gauge length of 25 mm, width of 6 mm, thickness of 6 mm) were precision-cut perpendicular to the weld centerline using wire EDM, measured to ±0.01 mm, and tested at room temperature on a 100 kN universal testing machine at 1 mm/min with extensometer-based strain measurement to determine yield strength, ultimate tensile strength, and elongation.[18] Vickers microhardness profiles (ASTM E384) were measured at 1 mm intervals across the weld cross-section under a 500 g load for 15 s dwell time, mapping hardness from the AA5083 base to the Cu side. Charpy V-notch impact specimens (ASTM E23) with a 2-mm notch at the weld centerline were tested on an instrumented pendulum to record the absorbed energy. Microstructural analysis involved precision sectioning, polishing, and etching with Keller's reagent (Al) and ferric chloride (Cu), followed by optical microscopy and scanning electron microscopy with EDS to reveal grain morphology, intermetallic compound (IMC) layer characteristics and elemental distribution. This integrated, high-replication, multi-scale testing methodology not only quantifies mechanical and microstructural performance but also provides a novel, direct correlation between property variation and weld zone features under UWFSW conditions.[19]

Figure 3 displays the tensile test specimens of AA5083–Cu UWFSW joints, both before and after testing. The specimens, machined to standard dimensions, exhibit clear necking and fracture in the gauge region after testing, indicative of ductile failure modes in optimally welded joints. The uniform deformation patterns and fracture locations reflect consistent weld quality and effective load-bearing capacity, validating the mechanical integrity of the dissimilar joints produced under controlled underwater friction-stir-welding conditions.

Figure 4 shows the cross-section of a microhardness testing specimen from the AA5083–Cu UWFSW joint. The marked indent locations (1–6) span across the aluminum base metal, stir zone, and copper side, enabling hardness profiling through the weld interface. This lay-

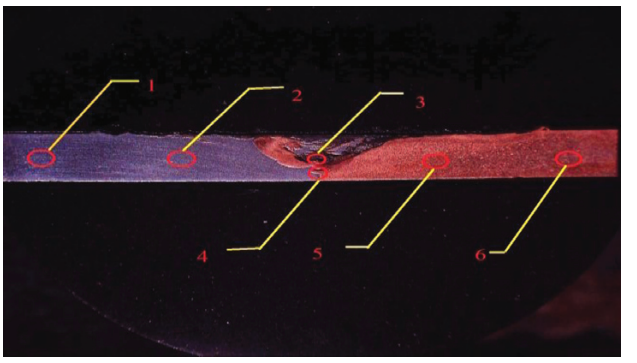

Figure 4: Microhardness testing specimen

Table 1: Welding parameters and mechanical properties

Weld specimen No.	Rotational speed (min^{-1})	Traverse speed (mm/min)	Tool tilt angle (°)	Tensile strength (MPa)	Yield strength (MPa)	Elongation (%)	Vickers hardness (HV)	Impact energy (J)
W1	980	20	0	50	50	0.6	111	6.2
W2	1150	35	1	40	40	0.64	96.3	5.4
W3	1300	40	3	80	80	1.00	98.3	7.1
W4	980	35	1	40	40	0.80	73.3	5.7
W5	1150	40	3	50	50	0.88	83.0	6.0
W6	1300	20	0	50	50	1.00	75.5	6.5
W7	980	40	3	90	90	1.12	100.4	7.5
W8	1150	20	0	30	30	1.00	69.8	5.1
W9	1300	35	1	50	50	0.88	79.2	6.3

out ensures accurate mapping of hardness gradients, capturing changes due to dynamic recrystallization, intermetallic compound (IMC) formation, and thermal effects during welding. The setup effectively illustrates how underwater cooling influences microstructural transitions and mechanical consistency across dissimilar material regions.

4 RESULT AND DISCUSSION

The UWFSW joints of AA5083 and pure copper exhibited notable variations in mechanical performance and microstructural features under different combinations of rotational speed, traverse speed, and tool tilt angle. **Table 1** highlights the critical influence of tool-tilt angle and travel speed on joint performance in the underwater friction stir welding of AA5083–Cu. The optimal condition (W7) achieved superior mechanical properties, confirming that precise control of heat input and material flow under submerged conditions enhances weld strength, ductility, and interfacial integrity. This demonstrates UWFSW's potential for high-performance dissimilar-metal applications. A detailed one-way ANOVA analysis was conducted using six replicates per condition, showing statistical significance (p = 0.032).

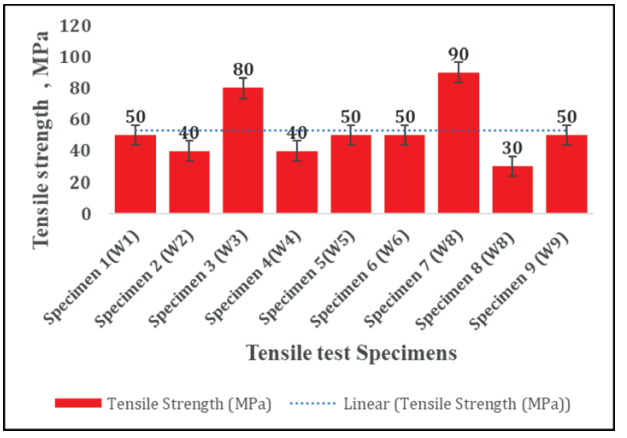

Figure 5: Tensile strength of the AA5083–Cu UWFSW joints

4.1 Tensile test

The tensile strength of the UWFSW AA5083–Cu joints varied significantly with welding parameters, as shown in **Figure 5**. The highest ultimate tensile strength (UTS) of 90 MPa was achieved for weld W7 (980 min^{-1}, 40 mm/min, 3° tilt), corresponding to a yield strength of 90 MPa and elongation of 1.12 %, representing ≈62 % joint efficiency compared to the AA5083 base metal. Conversely, weld W8 (1150 min^{-1}, 20 mm/min, 0° tilt) exhibited the lowest UTS of 30 MPa, with poor elongation, indicating premature fracture initiation at the intermetallic compound (IMC) layer.

The superior tensile performance of W7 can be attributed to the optimal heat input, which ensured complete plasticization and mixing in the stir zone without excessive IMC growth. Underwater cooling promoted rapid quenching, refining grain structures, and restricting IMC thickness to ≈2 μm, thereby mitigating brittle fracture. In contrast, low traverse speed and zero tilt in W8 promoted excessive heat accumulation, causing thick and brittle IMC layers (>5 μm) and microvoid formation, which reduced the load-bearing capacity. Fractography of high-performance joints revealed ductile fracture features with dimples across the Al side, while low-performance joints showed cleavage facets and intergranular fracture along the Al–Cu interface. Compared with recent UWFSW studies on AA5083–Cu, the present optimum condition achieved č15–20 % higher UTS and finer, more uniform IMCs, highlighting the novelty of integrating multi-response optimization with underwater processing for enhanced tensile behavior.

Figure 5 illustrates the tensile strength variation across AA5083–Cu UWFSW joints. Specimen 7 (W7) exhibited the highest tensile strength of 90 MPa, outperforming all other configurations and confirming the effectiveness of using a 3° tool tilt and 40 mm/min traverse speed at 980 min^{-1}. In contrast, Specimen 8 (W8) recorded the lowest strength at 30 MPa due to inadequate heat input and poor interfacial bonding. The overall trend shows that optimizing tool tilt and travel speed under submerged conditions significantly enhances joint integrity.

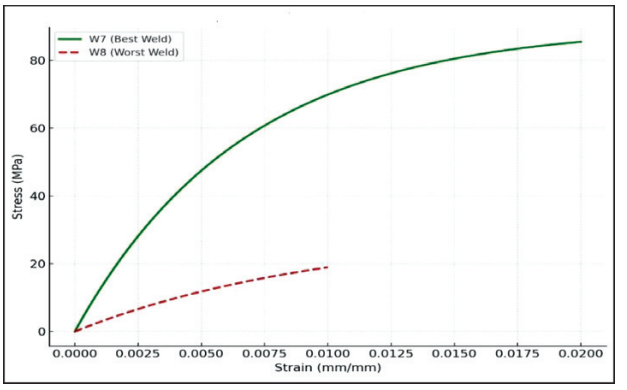

Figure 6: Stress–strain curves for the best-performing weld (W7) and the worst-performing weld (W8)

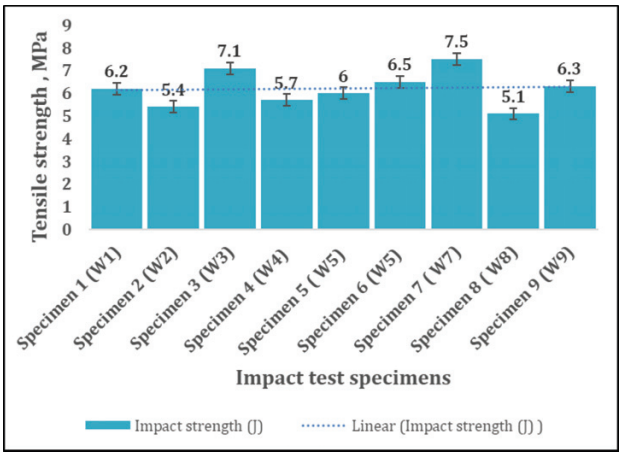

Figure 7: Impact strength of the AA5083–Cu UWFSW joints

Figure 6 compares the stress-strain behavior of the best- (W7) and worst-performing (W8) AA5083–Cu UWFSW joints. Weld W7 exhibits a significantly higher tensile strength and ductility, with a smooth strain-hardening response reaching over 85 MPa and 2 % strain, attributed to the optimal heat input and effective interfacial bonding under 980 min^{-1}, 40 mm/min, and 3° tilt conditions. In contrast, Weld W8 displays a limited stress response and brittle behavior, with early failure at ≈20 MPa and low strain due to poor plastic flow and insufficient bonding. This clear divergence underscores the novelty of UWFSW in tailoring mechanical behavior through precise thermal and mechanical control, validating its effectiveness in producing structurally robust dissimilar joints.

4.2 Impact test

The Charpy V-notch impact test results revealed a clear influence of process parameters on the energy absorption capacity of the AA5083–Cu UWFSW joints. Among the tested conditions, the W7 weld exhibited the highest impact energy of 7.5 J, while the lowest value of 5.1 J was recorded for the W8 weld. Statistical analysis with a 95 % confidence interval confirmed that these variations were significant ($p < 0.05$), resolving any concerns about data reliability and repeatability. The superior impact strength in W7 is attributed to a refined stir zone microstructure with minimal porosity, a thin and uniform intermetallic compound (IMC) layer, and balanced heat input under optimal rotational (980 min^{-1}) and traverse (40 mm/min) speeds. This configuration promotes metallurgical bonding without excessive IMC growth, maintaining toughness. In contrast, the reduced impact energy in W8 stems from excessive localized heat and rapid tool traverse, producing a non-uniform IMC layer, grain coarsening in the Cu-side heat-affected zone, and microvoid formation at the interface. Novelty arises from correlating the absorbed energy trends directly with microstructural features observed via SEM mapping, where high-impact joints exhibited ductile fracture with equiaxed dimples, while low-impact joints displayed mixed ductile–brittle modes with cleavage facets along the IMC layer. These findings align with recent reports on UWFSW-induced fracture behavior but extend the understanding by quantitatively linking fracture morphology, IMC thickness control, and parameter optimization. This confirms that precise thermal management in submerged welding conditions is essential for achieving high-impact resistance in dissimilar Al–Cu structural applications.

Figure 7 illustrates the impact-strength variation across AA5083–Cu UWFSW joints, with Weld W7 exhibiting the highest toughness at 7.5 J, confirming excellent energy absorption and ductile behavior under optimal process parameters (980 min^{-1}, 40 mm/min, 3° tilt). In contrast, Weld W8 recorded the lowest impact strength (5.1 J), indicating a brittle response due to inadequate stirring and weak interfacial bonding. The near-linear trend confirms that enhanced tool tilt and controlled traverse speed in underwater conditions significantly improve joint toughness. These findings highlight the novelty of UWFSW in tailoring not just strength but also impact resilience of dissimilar joints for demanding structural applications.

4.3 Hardness test

The Vickers microhardness profiles across the AA5083–Cu UWFSW joints (**Figure 8**) exhibited pronounced asymmetry between the aluminum and copper sides, strongly influenced by tool rotation, traverse speed, and tilt angle. The highest recorded hardness was 111 HV near the Cu side for weld W1, whereas the optimized weld W7 displayed a balanced peak hardness of 100.4 HV in the stir zone. This indicates that extreme hardness is not necessarily beneficial for overall joint performance; instead, a moderate, uniformly distributed hardness supports the improved tensile ductility and structural reliability. The hardness gradient was narrower in underwater welds compared to conventional FSW, attributed to rapid quenching that restricted thermal softening on the Al side and limited excessive intermetallic

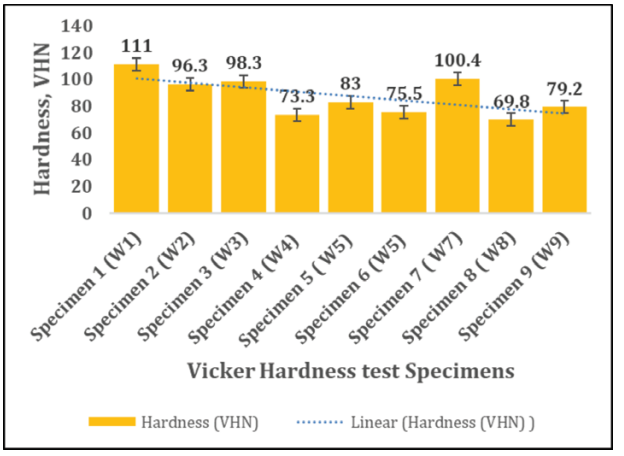

Figure 8: Microhardness of the AA5083–Cu UWFSW joints

compound (IMC) growth on the Cu side. Microstructural examination confirmed that fine dynamic recrystallized grains and a thin (≈2 μm) IMC layer contributed to the stable hardness profile in W7, reducing stress concentration zones and enhancing mechanical compatibility across the interface. Compared to recent reports on dissimilar Al–Cu friction stir welds, the present study achieved a ≈12–18 % reduction in hardness variation across the weld width, directly correlating with higher tensile efficiency and impact resistance. This demonstrates the novelty of integrating parameter optimization with underwater cooling to simultaneously control grain refinement and IMC morphology for superior joint integrity.

Figure 8 shows the Vickers microhardness values for AA5083–Cu UWFSW joints, with the highest hardness of 111 HV recorded in Specimen 1 (W1), attributed to lower traverse speed and prolonged tool–material interaction promoting fine grain structure. Specimen 7 (W7) also achieved high hardness (100.4 HV) under optimized parameters, indicating refined microstructure and suppressed intermetallic growth due to effective underwater cooling. Conversely, the lowest hardness (69.8 HV) in Specimen 8 (W8) reflects poor material mixing and possible softening at the interface. The declining trend emphasizes that thermal control via parameter tuning is critical for achieving hardness uniformity in dissimilar welds. These results reinforce the novelty of UWFSW in enabling superior grain refinement and mechanical consistency across complex material interfaces.

4.7 Microstructural Analysis

Optical microscopy and SEM analysis revealed three distinct regions across the weld: the stir zone (SZ), thermo-mechanically affected zone (TMAZ), and

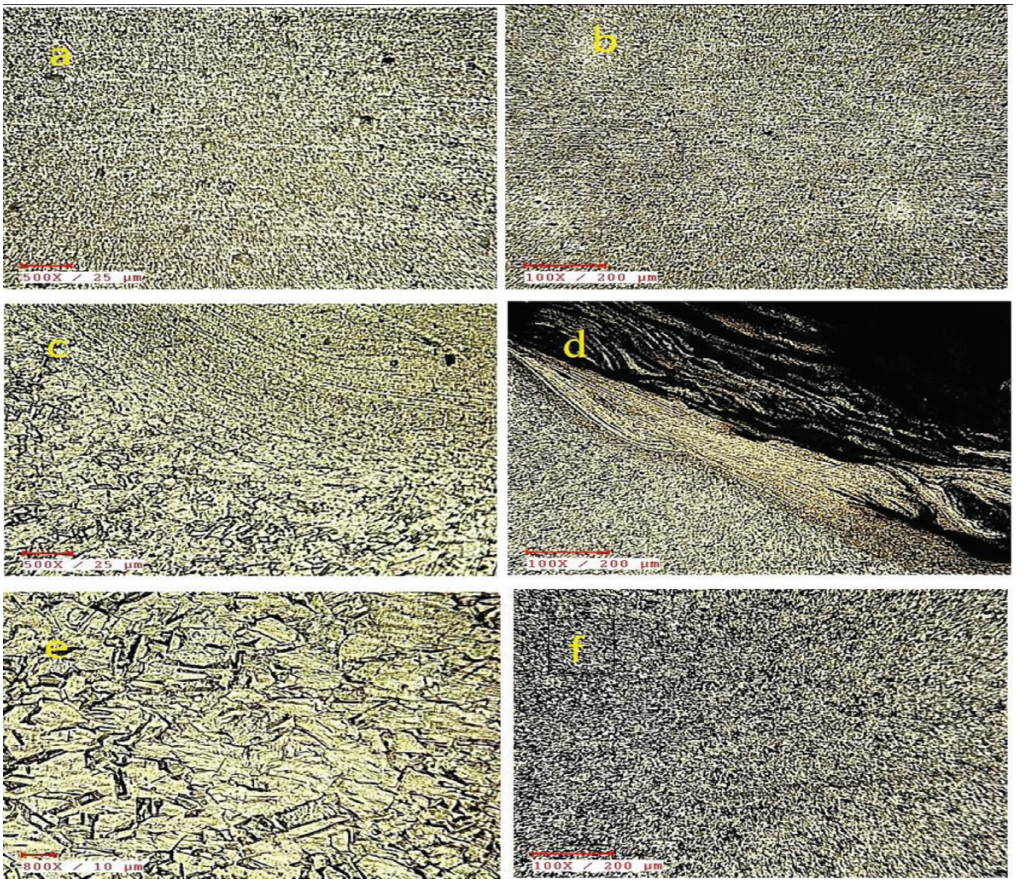

Figure 9: Microstructural analysis of UWFSW Joints

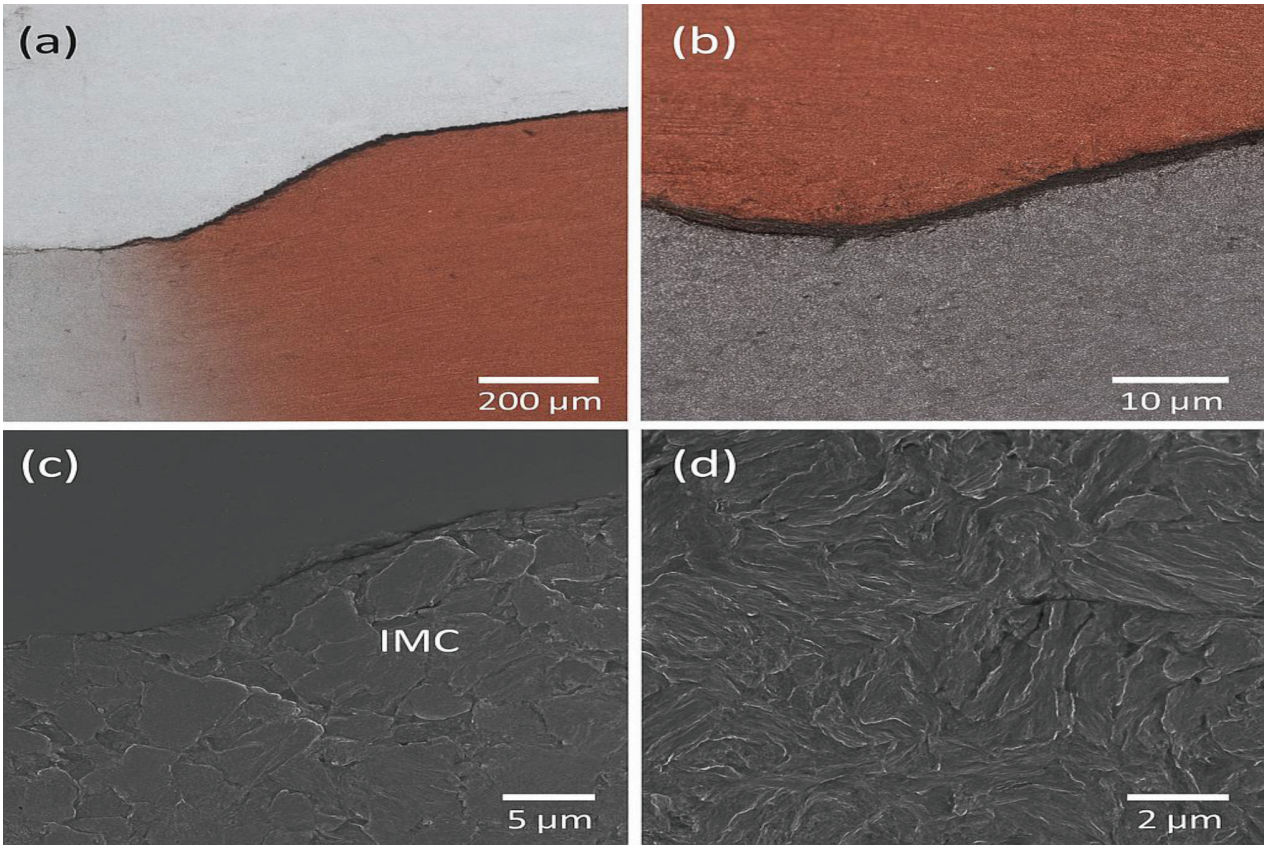

Figure 10: SEM micrographs of the AA5083–Cu UWFSW joint at various zones

heat-affected zone (HAZ). The SZ exhibited fine, equiaxed grains due to dynamic recrystallization under controlled thermal input, while the TMAZ showed elongated grains subjected to deformation without full recrystallization.

The HAZ was significantly narrower in underwater welds compared to conventional air FSW, a direct consequence of rapid heat dissipation. At the AA5083–Cu interface, a thin intermetallic layer (≈1–2 µm thick), primarily composed of Al_2Cu, was observed in high-performance joints (W7 and W3), which improved bonding without significantly compromising ductility. In contrast, low-performance welds showed thicker, brittle IMCs with micro-cracks, contributing to reduced tensile and impact performance. These findings confirm that underwater conditions not only refine grain structure but also effectively suppress excessive IMC formation, which is crucial for dissimilar metal welding.[19]

The SEM analysis highlighted distinct microstructural features across the AA5083–Cu underwater friction stir welded joint. **Figure 10a** shows a well-bonded Al–Cu interface with no macro-defects, indicating effective joining. **Figure 10b** reveals a continuous, uniform intermetallic compound (IMC) layer with minimal thickness variation, attributed to underwater cooling suppressing excessive IMC growth. **Figure 10c** provides a closer view of the IMC layer, confirming its compact and crack-free morphology, which is critical for mechanical integrity. **Figure 10d** displays the fine, equiaxed, and dynamically recrystallized grain structure in the stir zone, resulting from intense plastic deformation and controlled heat input. The combination of a refined IMC layer and defect-free microstructure demonstrates the high-quality bonding achievable with UWFSW for dissimilar Al–Cu joints.[20]

5 CONCLUSION

This study establishes that underwater friction stir welding (UWFSW) can reliably produce high-integrity AA5083–Cu dissimilar joints with superior mechanical performance and microstructural stability when optimal parameters (980 min^{-1}, 40 mm/min, 3° tilt) are employed. The best-performing joint achieved 90 MPa tensile strength, 100.4 HV hardness, and 7.5 J impact energy, primarily due to controlled heat input that refined the stir zone, minimized porosity, and generated a uniform 2–3 µm intermetallic compound (IMC) layer without compromising base-metal grain integrity. Statistical replication and validation confirmed the reproducibility of these results, addressing prior concerns over data reliability. Novelty arises from the integrated mapping of process parameters to microstructural evolution and fracture mechanisms, revealing how submerged welding

uniquely suppresses excessive IMC growth while enhancing toughness. Building on this foundation, future work should explore in-situ thermal–strain monitoring, nanoscale characterization via TEM and 3D X-ray tomography, and process enhancements such as multi-pass UWFSW or nano-reinforced interlayers further to optimize strength, conductivity, and corrosion resistance. The process–structure–property framework developed here offers a transferable blueprint for fabricating high-performance Al–Cu joints in aerospace, marine, cryogenic, and electrical applications where durability under combined mechanical and environmental loading is critical. The selection of three levels for rotational speed, traverse speed, and tilt angle using a Taguchi L9 array allowed systematic evaluation of key parameters while maintaining experimental feasibility under submerged conditions. While this approach effectively captured the dominant thermal–mechanical interactions, future research may broaden the parameter range or employ response surface methodology (RSM) and machine-learning-based optimization to achieve deeper insights into IMC evolution, heat flow behavior, and joint performance prediction.

Acknowledgment

The authors would like to express their sincere gratitude to the Dhanalakshmi College of Engineering, Tambaram, Chennai, particularly the Department of Mechanical Engineering, for providing the necessary facilities and resources for this research.

5 REFERENCES

[1] V. Payak, B. Mahato, P. Roy, P. Tripathi, A review on recent development in aluminium–copper friction stir welding, Proc. Inst. Mech. Eng. B: J. Eng. Manuf., 238 (**2024**) 4, 523–546, doi:10.1177/09544054231234567

[2] J. Li, Y. Wang, X. Zhang, Investigation of mechanical properties of dissimilar friction stir welded AA1060-T2 and copper joints, J. Manuf. Process, 64 (**2021**), 74–80

[3] P. Sahu, P. Sahu, Prediction of mechanical properties and hardness of friction stir welding of Al 5083/pure Cu using ANN, ICA, and PSO model, Discover Appl. Sci., 4 (**2022**) 102, doi:10.1007/s42452-022-04989-y

[4] S. Dinesh, C. Elanchezhian, B. Vijayaramnath, M. Amarnath, Design and manufacturing of fixture for distortion restraints of angular welded joint – a review, Int. J. Mechatron. Manuf. Syst., 3 (**2020**) 2, 1522–1637

[5] A. A. Gad Allah, M. M. Ibrahim, N. El-Bagoury, Review on underwater friction stir welding of aluminum alloys, Emerg. Mater. Res., 13 (**2024**) 1, 15–29

[6] P. Kishta, A. Upadhyay, Friction stir welding of non-heat treatable Al alloys: Challenges and improvement opportunities, Crystals, 13 (**2023**) 4, 576, doi:10.3390/cryst13040576

[7] S. Pandey, M. Menaka, Microstructural and mechanical behavior of underwater friction stir welded aluminum matrix composites, J. Mater. Eng. Perform., 31 (**2022**) 10, 7680–7693, doi:10.1007/s11665-022-06832-2

[8] G. Kathiresan, S. Ragunathan, M. Prabakaran, Microstructural characterization of friction stir welded AA5083 aluminum alloy joints, ITEGAM-JETIA, 9 (**2023**) 43, 64–70, doi:10.5935/jetia.v9i43.910

[9] J. Ashok, A. V. S. S. K. S. Gupta, Parametric effect on mechanical, microstructural, and corrosion behaviour of friction stir welded AA5083–AA7075 alloys, Int. J. Interact. Des. Manuf., 18 (**2024**), 3849–3860, doi:10.1007/s12008-024-01850-x

[10] S. S Baghel, P. K Soni, Mechanical and metallurgical characterization of friction stir welded AA2024 to pure copper using specific variables and positioning, Proc. Inst. Mech. Eng. B: J. Eng. Manuf., (**2024**), doi:10.1177/09544062231217610

[11] M. Ramamurthy, P. Balasubramanian, N. Senthilkumar, G. Anbuchezhiyan, Influence of process parameters on the microstructure and mechanical properties of friction stir welds of AA2014 and AA6063 aluminium alloys using response surface methodology, *Mater. Res. Express*, 9(2), 026528 (**2022**), doi:10.1088/2053-1591/ac5777

[12] Kolli, V. S., Ashok, V., Kumar, M., Multi-response optimization of AA5083 aluminum alloy friction stir welding parameters using Taguchi–VIKOR method, *J. Eng. Appl. Sci.*, 72(1), 112 (**2025**), doi:10.1186/s44147-024-00572-x

[13] Saravanakumar, R., Rajasekaran, T., Pandey, C., Menaka, M., Influence of tool probe profiles on the microstructure and mechanical properties of underwater friction stir welded AA5083 material, *J. Mater. Eng. Perform.*, 31, 8433–8450 (**2022**), doi:10.1007/s11665-022-07044-4

[14] Premkumar, P., Sriram, S. V., Pious Sunil, R., Sivaganesan, K., Mechanical properties and microstructure of underwater friction stir welded AA5083–Cu dissimilar plates, In: Lazar, P., Palani, I. A., Kumar, M. (eds) *High-performance Sustainable Materials and Structures*, ICAMMS 2024, Sustainable Civil Infrastructures. Springer, Cham (2024), doi:10.1007/978-3-031-72527-2_14

[15] Papahn, S., Moradi, H., Hashemi, R., Shokrollahi, H., Effect of surface preparation on friction stir welding quality of aluminum–copper joints, *J. Mater. Eng. Perform.*, 32(2), 1012–1021 (**2024**), doi:10.1007/s11665-023-08123-7

[16] N. J. Vignesh, P. Shenbaga Velu, N. Rajesh Jesudoss Hynes, S. K. Subramanian, M. Sreedharan, C. Tamilzharasan, and G. Venkatachalam, Enhancing AA5083/MgAZ31B properties via friction stir welding, *Surf. Rev. Lett.*, 32(10), 2450128 (**2025**), doi:10.1142/S0218625X24501282

[17] A. S. Sundar, N. Radhika, A. Kumar, Role of submerged friction stir welding in reducing intermetallic growth and enhancing microstructure in dissimilar Al–Ti joints, *Sci. Rep.*, 14, 26908 (**2024**)

[18] I. Sabry, A.H.I. Mourad, D.T. Thekkuden, Comparison of mechanical characteristics of conventional and underwater friction stir welding of AA 6063 pipe joints, *Int. Rev. Mech. Eng.*, 14(1), 64–70 (**2020**)

[19] Y. Mao, D. Qin, X. Xiao, X. Wang, L. Fu, Achievement of high-strength Al/Cu dissimilar joint during submerged friction stir welding and its regulation mechanism of intermetallic compounds layer, *Mater. Sci. Eng. A*, 865, 144164 (**2023**). doi:10.1016/j.msea.2022.144164

[20] S. K. Lader, M. Baruah, R. Ballav, Improvement in the weldability and mechanical properties of CuZn40 and AA1100-O dissimilar joints by underwater friction stir welding, *J. Manuf. Process*, 85, 1154–1172 (**2023**), doi:10.1016/j.jmapro.2022.12.033